Vol 454|7 August 2008|doi:10.1038/nature07091

LETTERS

Essential roles of PI(3)K–p110β in cell growth, metabolism and tumorigenesis

Shidong Jia[1,3]*, Zhenning Liu[1,3]*, Sen Zhang[1,3]*, Pixu Liu[1,3]*, Lei Zhang[1,3], Sang Hyun Lee[1,3], Jing Zhang[1,3], Sabina Signoretti[2,4], Massimo Loda[2,4], Thomas M. Roberts[1,3] & Jean J. Zhao[1,3,5]

On activation by receptors, the ubiquitously expressed class IA isoforms (p110α and p110β) of phosphatidylinositol-3-OH kinase (PI(3)K) generate lipid second messengers, which initiate multiple signal transduction cascades[1–5]. Recent studies have demonstrated specific functions for p110α in growth factor and insulin signalling[6–8]. To probe for distinct functions of p110β, we constructed conditional knockout mice. Here we show that ablation of p110β in the livers of the resulting mice leads to impaired insulin sensitivity and glucose homeostasis, while having little effect on phosphorylation of Akt, suggesting the involvement of a kinase-independent role of p110β in insulin metabolic action. Using established mouse embryonic fibroblasts, we found that removal of p110β also had little effect on Akt phosphorylation in response to stimulation by insulin and epidermal growth factor, but resulted in retarded cell proliferation. Reconstitution of p110β-null cells with a wild-type or kinase-dead allele of p110β demonstrated that p110β possesses kinase-independent functions in regulating cell proliferation and trafficking. However, the kinase activity of p110β was required for G-protein-coupled receptor signalling triggered by lysophosphatidic acid and had a function in oncogenic transformation. Most strikingly, in an animal model of prostate tumour formation induced by *Pten* loss, ablation of *p110β* (also known as *Pik3cb*), but not that of *p110α* (also known as *Pik3ca*), impeded tumorigenesis with a concomitant diminution of Akt phosphorylation. Taken together, our findings demonstrate both kinase-dependent and kinase-independent functions for p110β, and strongly indicate the kinase-dependent functions of p110β as a promising target in cancer therapy.

Class IA PI(3)Ks are heterodimeric lipid kinases consisting of a p110 catalytic subunit complexed to one of several regulatory subunits, collectively called p85 (refs 4, 5). In response to stimulation by growth factor, p110 subunits catalyse the production of the lipid second messenger phosphatidylinositol-3,4,5-trisphosphate ($PtdIns(3,4,5)P_3$) at the membrane[1–4]. This second messenger in turn activates the serine/threonine kinase Akt and other downstream effectors[9,10]. Knockout mice for either *p110α* or *p110β* die early in embryonic development[11,12]. However, recent studies using conditional knockout strategies[8] and isoform-specific small molecule inhibitors[7] showed that p110α is important in growth-factor signalling, whereas a kinase-inactive knock-in mouse model showed that insulin responses depended on the catalytic activity of p110α (ref. 6).

To investigate the role(s) of p110β in cell, tissue and organismal physiology and to examine it as a potential therapeutic target in cancer, we generated mice carrying a conditional *Pik3cb* allele (Supplementary Fig. 1). We first investigated the role of p110β in insulin action. Because liver is the major insulin-responsive organ, we examined the effects of p110β loss on hepatic insulin function. To achieve liver-specific deletion of *p110β*, we injected the tail veins of $p110\beta^{flox/flox}$ mice with adenoviruses expressing β-galactosidase (Ade-LacZ) or Cre recombinase (Ade-Cre) to generate matched cohorts of control mice and mice with hepatocyte-specific deletion of *p110β*. Additional cohorts of wild-type animals were subjected to Ade-Cre or Ade-LacZ, allowing us to rule out potential non-specific Cre effects (data not shown). A more than 90% decrease in p110β protein was seen in the livers of Ade-Cre-injected mice, whereas *p110β* expression remained unchanged in the livers of the control mice and muscle tissues from both groups as measured by western blotting (Supplementary Fig. 2a, b). Consistent with previous findings[6,7] that the kinase activity of p110β has only a minor function in insulin signalling, we saw no significant change in Akt phosphorylation in response to insulin challenge in livers lacking p110β (Supplementary Fig. 2a). However, mice deficient in hepatic p110β had higher levels of insulin in the blood than control animals when fasted (Fig. 1a). These animals also showed a lower tolerance of glucose and sensitivity to insulin on challenge by intraperitoneal injection of glucose or insulin (Fig. 1b, c). Mice deficient in hepatic p110β produced more glucose than control animals did in a pyruvate challenge test (Fig. 1d). An analysis of lipogenesis showed no significant changes in serum triglycerides, fatty acids and cholesterol levels when *p110β* was deleted from liver (Supplementary Fig. 3), but leptin levels were elevated compared with those in control animals, as was seen in p110α kinase-dead knock-in animals[6] (Supplementary Fig. 3). Of a panel of gluconeogenic genes, only that encoding phosphoenolpyruvate carboxykinase (PEPCK) was increased in p110β-deficient livers (Supplementary Fig. 4). PEPCK promotes the production and synthesis of glucose in liver, resulting in a greater release of glucose into blood. This result therefore provides at least a partial explanation for the metabolic phenotypes observed. Although these findings indicate that p110β might contribute to metabolic regulation through a kinase-independent mechanism, we cannot rule out the involvement of the catalytic role of p110β in insulin responses. Our observations are in line with earlier work[7] in which a p110β-specific small-molecule inhibitor was used to demonstrate that acute blockage of the kinase activity of p110β had little effect on insulin action. In addition, another study[13] found that mice doubly heterozygous for knockout of *p110α* and *p110β* showed decreased sensitivity to insulin with no apparent changes in Akt phosphorylation.

To obtain cells for detailed signalling studies, mouse embryonic fibroblasts (MEFs) were isolated from floxed embryos and their wild-type littermates, as described in Supplementary Information (Supplementary Fig. 5a–c). MEFs lacking p110β proliferated significantly more slowly than parental ($p110\beta^{flox/flox}$) or wild-type

[1]Department of Cancer Biology and [2]Department of Medical Oncology, Dana-Farber Cancer Institute, Boston, Massachusetts 02115, USA. [3]Department of Pathology and [4]Department of Pathology and [5]Department of Surgery, Brigham and Women's Hospital, Harvard Medical School, Boston, Massachusetts 02115, USA.
*These authors contributed equally to this work.

($p110\beta^{+/+}$ after Cre) MEFs (Fig. 2a). To obtain a second, more easily renewed supply of knockout cells, we established immortalized $p110\beta^{flox/flox}$ and $p110\beta^{+/+}$ MEFs by means of infection with a retrovirus encoding a dominant-negative form of p53 (DNp53)[14]. We also generated an add-back line by introducing haemagglutinin (HA)-tagged human p110β to DNp53-immortalized $p110\beta^{flox/flox}$ MEFs. These immortalized MEFs were then treated with Ade-Cre to yield the following MEF lines: βKO (from $p110\beta^{flox/flox}$) and βKO+β (from the add-back). For wild-type control MEFs, designated WT, we used DNp53-immortalized $p110\beta^{flox/flox}$ cells without Cre treatment interchangeably with Cre-treated DNp53-immortalized $p110\beta^{+/+}$ MEFs, because no significant differences were ever seen between these two possible controls. Deletion of *p110β* had no obvious negative effect on the phosphorylation of Akt in either primary MEFs or DNp53-immortalized MEFs in response to stimulation by insulin, epidermal growth factor (EGF) and platelet-derived growth factor (Fig. 2c and Supplementary Fig. 6a–c). However, a moderate diminution in the phosphorylation of the S6 ribosomal protein (S6RP) at Ser 235/Ser 236 was detected in these βKO cells in response to insulin or serum (Supplementary Fig. 7). Previous studies have implicated p110β in signalling elicited by G-protein-coupled receptors (GPCRs)[15,16]. We found consistently that both phospho-Akt and phospho-S6RP levels were decreased in response to lysophosphatidic acid (LPA) in cells lacking p110β (Fig. 2d and Supplementary Fig. 8a).

To dissect the potential kinase-dependent and kinase-independent roles of p110β, we reconstituted βKO MEFs with a kinase-inactive allele of HA-tagged human *p110β*, using the previously reported K805R mutation (KR)[17] to generate the βKO+KR MEF line. Though the expression of KR was lower than that of the WT add-back construct, it was expressed at a level slightly higher than endogenous p110β, and expression levels of p110α were unchanged (Supplementary Fig. 9a, and data not shown). Loss of lipid kinase activity in the KR cells was confirmed by lipid kinase assay[8,18] after immunoprecipitation with anti-p110β (Supplementary Fig. 9b). We then examined the effect of WT or KR add-back on the altered signalling seen after the loss of p110β. The decrease in both phospho-Akt and phospho-S6RP in response to stimulation with LPA observed in βKO cells was restored by adding back WT but not the KR allele of *p110β* (Fig. 2d and Supplementary Fig. 8b), suggesting a catalytic function for p110β in LPA signalling. This seems to be unique to p110β, because loss of p110α has no obvious effect on LPA signalling (Fig. 2e). The lower phospho-S6RP levels in βKO cells were restored by both WT and KR add-backs in response to insulin or fetal bovine serum (FBS) (Supplementary Fig. 7, and data not shown), suggesting a scaffolding role of p110β in signalling by insulin and growth factors. However, our MEF data do not rule out a role for p110β in classical signalling by PI(3)K in other circumstances. For instance, when we ablated *p110α* in our earlier work, residual phosphorylation by Akt was observed in response to growth factors[8]. Because MEFs express *p110α* and *p110β* and not other class I PI(3)Ks, this residual signal was presumably transduced by p110β. We also note that *p110β* ablation removes the protein as a competitor for p110α on receptors, which may allow any decrease in signalling caused by p110β loss to be masked or compensated for by an increased signal flux through p110α.

To test the kinase-dependent and/or kinase-independent effects of p110β on cell proliferation, we studied cell cycle kinetics by first synchronizing cells by serum starvation and then measuring the proportion of cells in S phase with the incorporation of bromodeoxyuridine (BrdU) after re-feeding. Whereas βKO cells had a delayed peak of BrdU incorporation, KR reconstituted cells showed a similar incorporation of BrdU to that of WT and βKO+β cells (Fig. 2f).

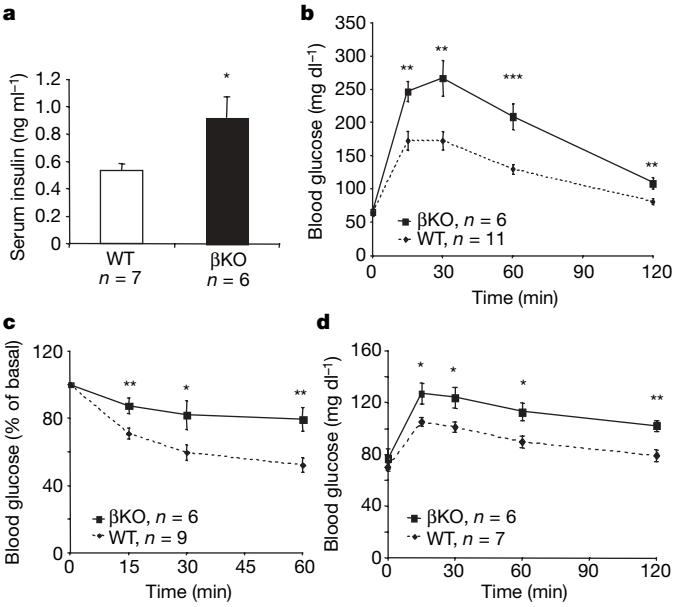

Figure 1 | Mice with liver-specific deletion of *p110β* show resistance to insulin and intolerance of glucose. Mice 8–10 weeks old were injected with adenoviruses expressing LacZ or Cre recombinase. Two weeks after injection, metabolism was analysed as follows: fasted serum insulin levels (**a**); glucose tolerance test (**b**); insulin tolerance test (**c**) (results represent blood glucose concentrations as a percentage of starting value at time zero); pyruvate challenge (**d**). Data are shown as means and s.e.m. Asterisk, $P < 0.05$; two asterisks, $P < 0.01$; three asterisks, $P < 0.001$ (*t*-test).

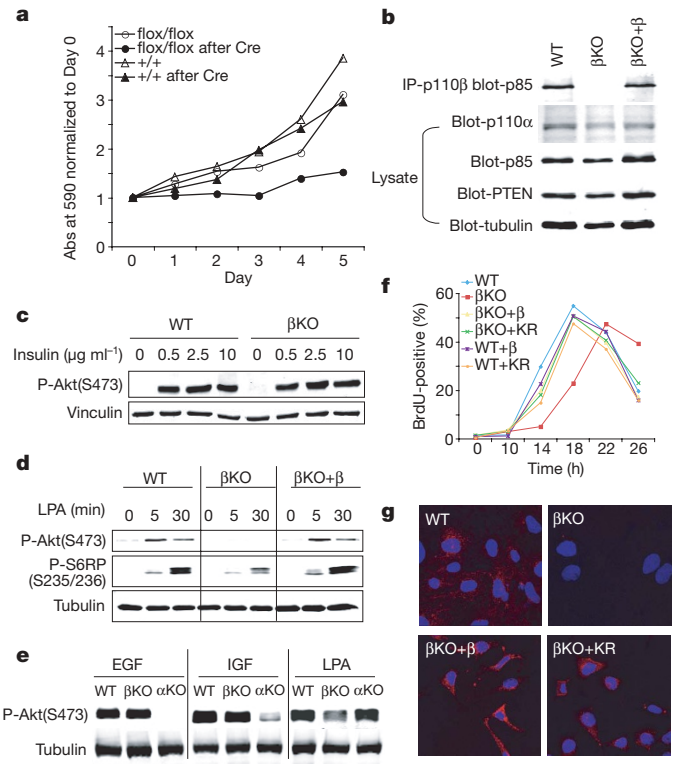

Figure 2 | Analyses of the effects of *p110β* deletion on cell growth and signalling. **a**, Loss of p110β retards cell growth of primary MEFs. Representative data are shown from triplicate experiments. **b**, Loss of endogenous p110β protein in immortalized MEFs. IP, immunoprecipitation. **c**, Loss of p110β has no negative effect on insulin signalling. **d**, Loss of p110β impairs LPA-induced signalling. **e**, Comparison of the responses of αKO, βKO and WT MEFs to stimulation with EGF, insulin-like growth factor (IGF) or LPA. **f**, BrdU incorporation assay. **g**, Transferrin uptake in various MEF lines is shown as indicated. Transferrin is labelled red and 4,6-diamidino-2-phenylindole blue.

Consistently, βKO+KR MEFs showed proliferation rates similar to those of WT and βKO+β cells (Supplementary Fig. 9c), suggesting a kinase-independent role of p110β in cell proliferation.

Because previous studies have found p110β associated with members of the Rab family of small G proteins and clathrin-coated vesicles[19], we measured transferrin uptake in βKO MEFs and found it to be defective compared with that in WT and βKO+β MEFs (Fig. 2g). Interestingly, normal uptake of transferrin was restored by the KR construct (Fig. 2g). Although there is ample published evidence indicating the importance of transferrin uptake for the growth of a variety of cell types[20], it is not clear whether the defect in transferrin uptake is a primary cause of the growth defect observed here.

Class IA PI(3)Ks have been clearly implicated in cancer[21–24], with much recent work delineating the role of p110α in cancer[25–27]. To study a potential role of p110β in oncogenic transformation, we performed focus formation assays by infecting monolayers of DNp53-immortalized MEFs with retroviruses expressing various oncogenes. Oncogenic HRas-G12V and EGFR-Del (ΔL747–E749, A750P) retroviruses efficiently raised foci in WT cells but failed to transform βKO MEFs (Fig. 3a). The decreases in foci seen in βKO MEFs were actually more pronounced than those seen in *p110α* KO MEFs (Supplementary Fig. 10). Transformation was fully restored in βKO+β cells but partly restored in βKO+KR cells (Fig. 3a), suggesting that both the kinase activity and kinase-independent functions of p110β may have a function in oncogene-induced transformation.

PTEN, a lipid phosphatase, functions to oppose class IA PI(3)K kinase activity. Loss of *Pten* expression is a common event in many solid tumours[28]. The key challenge is to identify which p110 isoform's catalytic activity is unshackled by *Pten* loss in any given tumour. To test for a role of *p110β* in tumorigenesis driven by *Pten* loss, we generated mice that carried the $Pten^{flox/flox}$ (ref. 29) and $p110\beta^{flox/flox}$ alleles, as well as a probasin-driven Cre transgene[30], to specifically delete *Pten* and *p110β* in prostatic epithelium. Prostates had a normal appearance in the absence of p110β (Fig. 3b, c). Prostate tissue lacking *Pten* expression showed universal high-grade prostatic intraepithelial neoplasia in the anterior lobe by 12 weeks. Ablation of *p110β* blocked the tumorigenesis caused by *Pten* loss in the anterior prostate (Table 1 and Fig. 3b, c). The loss of *Pten* was confirmed by genomic DNA analysis after laser-capture-assisted microdissection of single epithelial layers and by western blotting (Supplementary Fig. 11, and data not shown). Whereas Cre-mediated loss of *Pten* efficiently activated Akt in the prostate as judged by its phosphorylation on Ser 473, additional ablation of *p110β* diminished the phospho-Akt levels (Fig. 3b), suggesting that p110β catalytic activity contributes to tumorigenesis. More surprisingly, when we performed the same set of experiments using *p110α* ablation, we saw no changes either in tumour formation or in Akt phosphorylation (Table 1 and Fig. 3b, c). Again, the complete excision of *p110α* in tumour tissues was confirmed by multiple measures (Supplementary Fig. 12, and data not shown). It has been suggested that p110α and p110β generate distinct pools of PtdIns(3,4,5)P_3 (ref. 7). In response to insulin or other stimuli, an acute flux of PtdIns(3,4,5)P_3 is produced largely by p110α and is efficiently coupled to Akt phosphorylation. In contrast, p110β has been proposed to generate a basal level of PtdIns(3,4,5)P_3 with little effect on Akt phosphorylation[7]. It was shown that Akt phophorylation induced by *Pten* loss *in vitro* was sensitive to p110β-specific inhibitors[7]. We propose that it is this basal PtdIns(3,4,5)P_3 signal that has been enhanced to drive transformation and Akt activation by *Pten* loss in the murine prostate (Fig. 3d). Alternatively, the differential effects of *p110α* and *p110β* ablation may arise because the signal activating PI(3)K is generated by an as yet unidentified GPCR or a receptor tyrosine kinase that functions through p110β.

Thus, our data suggest distinct functions for p110β and p110α in cell signalling and transformation. We have showed that p110β has an important physiological function in metabolic regulation and glucose homeostasis, perhaps involving a kinase-independent mechanism. A kinase-independent function of p110β was further suggested in controlling cell proliferation and trafficking in *p110β* KO MEFs and MEFs reconstituted with a WT or kinase-dead allele of *p110β*. It would clearly be a mistake to overlook the contributions of p110β as a kinase. The basal PtdIns(3,4,5)P_3 pool catalysed by p110β seems to be 'silent' in response to stimulation by insulin and other growth factors, but becomes a 'powerhouse' to drive oncogenic

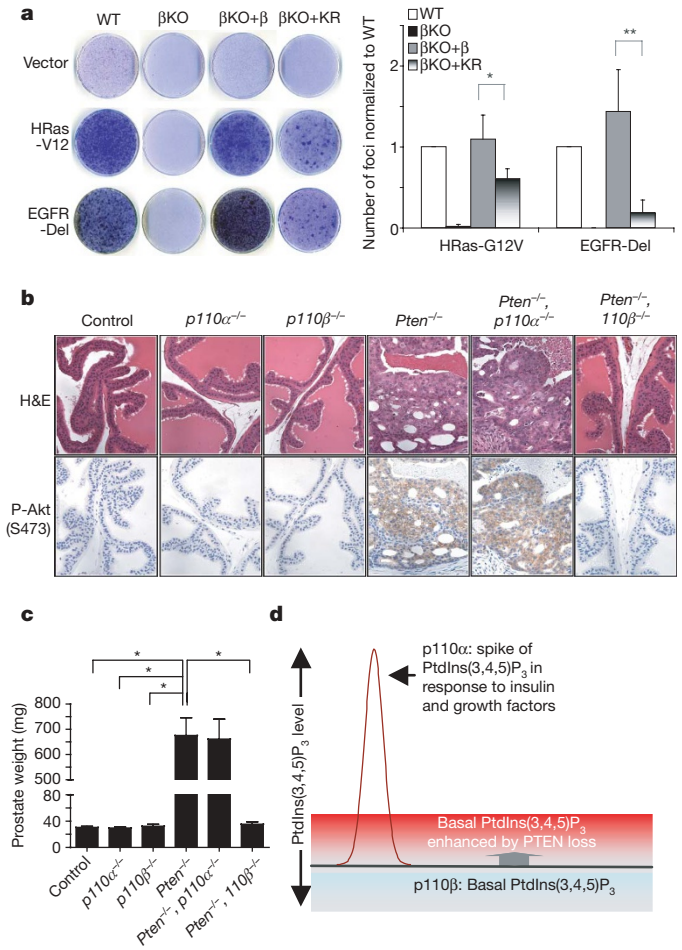

Figure 3 | Kinase activity of p110β contributes to transformation both *in vitro* and *in vivo*. **a**, Focus formation assay in KO and reconstituted MEFs. Results are shown as means and s.e.m. for four independent experiments (asterisk, $P < 0.05$; two asterisks, $P < 0.01$, *t*-test). **b**, Effects of *p110β* or *p110α* ablation on tumorigenesis caused by PTEN loss in the anterior prostate. **c**, Quantification of the weight (means and s.e.m.) of anterior prostate tissues of the indicated strain ($n = 10$ per group; asterisk, $P < 0.001$, *t*-test). **d**, A model for the elevation of basal PtdIns(3,4,5)P_3 signals derived from p110β catalytic activity induced by PTEN loss.

Table 1 | Effects of ablation of *p110α* or *p110β* on prostate tumorigenesis induced by PTEN loss

Abbreviation	Full name	Animals positive for PIN/ number of animals used
Control	Floxed littermates	0/20
$p110\alpha^{-/-}$	$p110\alpha^{flox/flox}$; PbCre4	0/20
$p110\beta^{-/-}$	$p110\beta^{flox/flox}$; PbCre4	0/14
$Pten^{-/-}$	$Pten^{flox/flox}$; PbCre4	20/20
$Pten^{-/-}$; $p110\alpha^{-/-}$	$Pten^{flox/flox}$; $p110\alpha^{flox/flox}$; PbCre4	15/15
$Pten^{-/-}$; $p110\beta^{-/-}$	$Pten^{flox/flox}$; $p110\beta^{flox/flox}$; PbCre4	0/16

Paraffin sections of anterior prostates from the indicated strains at 12 weeks were stained with haematoxylin/eosin. The pathological phenotype was uniformly observed within each genotype and is summarized in the table. PIN, prostatic intraepithelial neoplasia.

transformation in the absence of PTEN, as evident in our mouse prostate tumour model. Taken together, our findings indicate that p110β may be an attractive target for kinase inhibitors in cancer treatment with minor metabolic disturbances.

METHODS SUMMARY

Mice carrying floxed *p110β* (generated in this work), floxed *p110α* (ref. 8), floxed *Pten*[29] and probasin-driven Cre transgene[30] (Mouse Models of Human Cancers Consortium (MMHCC), National Cancer Institute) were used in this study. All animals were housed and treated in accordance with protocols approved by the Institutional Animal Care and Use Committees of Dana-Farber Cancer Institute and Harvard Medical School. The generation, culture and immortalization of MEFs, growth factor signalling study, retroviral infection, cell growth, cell cycle, lipid kinase assay, transferrin internalization, focus formation, glucose tolerance testing, insulin tolerance tests, pyruvate challenge, immunoprecipitation, immunoblotting, immunohistochemical and histological analyses were performed in accordance with standard or published protocols. Statistical analyses were performed with Student's *t*-test unless otherwise indicated.

Full Methods and any associated references are available in the online version of the paper at www.nature.com/nature.

Received 27 February; accepted 15 May 2008.
Published online 25 June 2008.

1. Vanhaesebroeck, B. & Waterfield, M. D. Signaling by distinct classes of phosphoinositide 3-kinases. *Exp. Cell Res.* **253,** 239–254 (1999).
2. Blume-Jensen, P. & Hunter, T. Oncogenic kinase signalling. *Nature* **411,** 355–365 (2001).
3. Vivanco, I. & Sawyers, C. L. The phosphatidylinositol 3-kinase AKT pathway in human cancer. *Nature Rev. Cancer* **2,** 489–501 (2002).
4. Engelman, J. A., Luo, J. & Cantley, L. C. The evolution of phosphatidylinositol 3-kinases as regulators of growth and metabolism. *Nature Rev. Genet.* **7,** 606–619 (2006).
5. Liu, Z. & Roberts, T. M. Human tumor mutants in the p110α subunit of PI3K. *Cell Cycle* **5,** 675–677 (2006).
6. Foukas, L. C. *et al.* Critical role for the p110α phosphoinositide-3-OH kinase in growth and metabolic regulation. *Nature* **441,** 366–370 (2006).
7. Knight, Z. A. *et al.* A pharmacological map of the PI3-K family defines a role for p110α in insulin signaling. *Cell* **125,** 733–747 (2006).
8. Zhao, J. J. *et al.* The p110α isoform of PI3K is essential for proper growth factor signaling and oncogenic transformation. *Proc. Natl Acad. Sci. USA* **103,** 16296–16300 (2006).
9. Bader, A. G., Kang, S., Zhao, L. & Vogt, P. K. Oncogenic PI3K deregulates transcription and translation. *Nature Rev. Cancer* **5,** 921–929 (2005).
10. Vanhaesebroeck, B. *et al.* Synthesis and function of 3-phosphorylated inositol lipids. *Annu. Rev. Biochem.* **70,** 535–602 (2001).
11. Bi, L., Okabe, I., Bernard, D. J., Wynshaw-Boris, A. & Nussbaum, R. L. Proliferative defect and embryonic lethality in mice homozygous for a deletion in the p110α subunit of phosphoinositide 3-kinase. *J. Biol. Chem.* **274,** 10963–10968 (1999).
12. Bi, L., Okabe, I., Bernard, D. J. & Nussbaum, R. L. Early embryonic lethality in mice deficient in the p110β catalytic subunit of PI 3-kinase. *Mamm. Genome* **13,** 169–172 (2002).
13. Brachmann, S. M., Ueki, K., Engelman, J. A., Kahn, R. C. & Cantley, L. C. Phosphoinositide 3-kinase catalytic subunit deletion and regulatory subunit deletion have opposite effects on insulin sensitivity in mice. *Mol. Cell. Biol.* **25,** 1596–1607 (2005).
14. Shaulian, E., Zauberman, A., Ginsberg, D. & Oren, M. Identification of a minimal transforming domain of p53: negative dominance through abrogation of sequence-specific DNA binding. *Mol. Cell. Biol.* **12,** 5581–5592 (1992).
15. Hazeki, O. *et al.* Activation of PI 3-kinase by G protein βγ subunits. *Life Sci.* **62,** 1555–1559 (1998).
16. Roche, S., Downward, J., Raynal, P. & Courtneidge, S. A. A function for phosphatidylinositol 3-kinase β (p85α-p110β) in fibroblasts during mitogenesis: requirement for insulin- and lysophosphatidic acid-mediated signal transduction. *Mol. Cell. Biol.* **18,** 7119–7129 (1998).
17. Yart, A. *et al.* A function for phosphoinositide 3-kinase β lipid products in coupling βγ to Ras activation in response to lysophosphatidic acid. *J. Biol. Chem.* **277,** 21167–21178 (2002).
18. Nobukuni, T. *et al.* Amino acids mediate mTOR/raptor signaling through activation of class 3 phosphatidylinositol 3OH-kinase. *Proc. Natl Acad. Sci. USA* **102,** 14238–14243 (2005).
19. Shin, H. W. *et al.* An enzymatic cascade of Rab5 effectors regulates phosphoinositide turnover in the endocytic pathway. *J. Cell Biol.* **170,** 607–618 (2005).
20. Daniels, T. R., Delgado, T., Rodriguez, J. A., Helguera, G. & Penichet, M. L. The transferrin receptor part I: Biology and targeting with cytotoxic antibodies for the treatment of cancer. *Clin. Immunol.* **121,** 144–158 (2006).
21. Bellacosa, A. *et al.* Molecular alterations of the AKT2 oncogene in ovarian and breast carcinomas. *Int. J. Cancer* **64,** 280–285 (1995).
22. Li, J. *et al.* PTEN, a putative protein tyrosine phosphatase gene mutated in human brain, breast, and prostate cancer. *Science* **275,** 1943–1947 (1997).
23. Steck, P. A. *et al.* Identification of a candidate tumour suppressor gene, MMAC1, at chromosome 10q23.3 that is mutated in multiple advanced cancers. *Nature Genet.* **15,** 356–362 (1997).
24. Ringel, M. D. *et al.* Overexpression and overactivation of Akt in thyroid carcinoma. *Cancer Res.* **61,** 6105–6111 (2001).
25. Samuels, Y. *et al.* High frequency of mutations of the PIK3CA gene in human cancers. *Science* **304,** 554 (2004).
26. Zhao, J. J. *et al.* The oncogenic properties of mutant p110α and p110β phosphatidylinositol 3-kinases in human mammary epithelial cells. *Proc. Natl Acad. Sci. USA* **102,** 18443–18448 (2005).
27. Bader, A. G., Kang, S. & Vogt, P. K. Cancer-specific mutations in PIK3CA are oncogenic *in vivo*. *Proc. Natl Acad. Sci. USA* **103,** 1475–1479 (2006).
28. Chen, Z. *et al.* Crucial role of p53-dependent cellular senescence in suppression of Pten-deficient tumorigenesis. *Nature* **436,** 725–730 (2005).
29. Lesche, R. *et al.* Cre/loxP-mediated inactivation of the murine Pten tumor suppressor gene. *Genesis* **32,** 148–149 (2002).
30. Wu, X. *et al.* Generation of a prostate epithelial cell-specific Cre transgenic mouse model for tissue-specific gene ablation. *Mech. Dev.* **101,** 61–69 (2001).

Supplementary Information is linked to the online version of the paper at www.nature.com/nature.

Acknowledgements We thank C. D. Stiles and J. D. Iglehart for advice, and H. Wu for providing floxed PTEN mice. This work was supported by grants from the National Institutes of Health (M.L., T.M.R. and J.J.Z.,), the Department of Defense for Cancer Research (J.J.Z.), the V Foundation (J.J.Z.) and the Claudia Barr Program (J.J.Z.). In compliance with Harvard Medical School guidelines, we disclose the consulting relationships: Novartis Pharmaceuticals, Inc. (M.L., T.M.R. and J.J.Z.).

Author Contributions Z.L., S.Z. and S.L. generated the floxed *p110β* mouse. S.J. carried out mouse tumorigenesis studies. Z.L and S.Z. performed MEF studies. P.L. performed *in vivo* metabolic studies. L.Z. performed transferrin uptake assays. J.Z. assisted in focus formation and BrdU incorporation experiments. S.S. and M.L. performed and interpreted pathological analyses of mouse prostate tumors. T.M.R. and J.J.Z. supervised the research, interpreted the data and wrote the paper. S.J., Z.L., S.Z., P.L., L.Z., S.L. and M.L. participated in the writing of the paper.

Author Information Reprints and permissions information is available at www.nature.com/reprints. Correspondence and requests for materials should be addressed to T.M.R. (thomas_roberts@dfci.harvard.edu) or J.J.Z. (jean_zhao@dfci.harvard.edu)

METHODS

Mice for metabolic and tumour studies. Conditional knockout mice of *p110β* were generated using the Cre-LoxP system. In brief, the targeting construct was assembled by isolating a 7.5-kilobase genomic fragment of *Pik3cb* from 129SvEv mouse strain and inserting two LoxP sites to flank exon 2 of *Pik3cb*. The targeting construct was electroporated into embryonic stem (ES) cells of 129SvEv mouse. ES clones carrying floxed *Pik3cb* were injected into the blastocysts of C57BL/6 mice. Male chimaeras were bred to C57BL/6 females to establish germline transmission of the conditional allele. The resulting heterozygous line ($p110\beta^{flox/+}$) was intercrossed to yield a homozygous line ($p110\beta^{flox/flox}$).

For metabolic studies, 8–10-week-old male $p110\beta^{flox/flox}$ littermates were tail-vein injected with 75 μl of adenovirus CMV-lacZ and CMV-cre (titre between 10^{10} and 4×10^{10} plaque-forming units ml^{-1}; University of Iowa Gene Transfer Vector Core). Two weeks after injection of adenoviruses, glucose tolerance test, insulin tolerance test, pyruvate challenge and *in vivo* insulin signalling were performed as described previously[31]. Blood glucose values were determined with an Accu-Chek AVIVA glucose monitor (Roche). Serum insulin and leptin (Crystal Chem Inc.), serum-free fatty acids and triacylglycerols (Wako) and serum cholesterol (Thermo) were measured by ELISA in accordance with the manufacturer's instructions.

It took two steps to generate compound mice for tumour studies. All floxed mice used were originally in the 129-C57BL/6 background and had been back-crossed once to C57BL/6. The probasin Cre mice were in the C57BL/6 background. In step 1, male PbCre4 mice were first crossed to the female $Pten^{flox/flox}$, $p110\alpha^{flox/flox}$ or $p110\beta^{flox/flox}$ mice, and the male offspring carrying PbCre4 were then crossed to female $Pten^{flox/flox}$, $p110\alpha^{flox/flox}$ or $p110\beta^{flox/flox}$ mice to obtain $Pten^{flox/flox}$; PbCre4 (hereafter termed '$Pten^{-/-}$'), $p110\alpha^{flox/flox}$; PbCre4 (hereafter termed '$p110\alpha^{-/-}$') or $p110\beta^{flox/flox}$; PbCre4 (hereafter termed '$p110\beta^{-/-}$') mice, respectively. We used cohorts of littermates lacking the probasin Cre transgene as wild-type controls ($Pten^{flox/flox}$, $p110\alpha^{flox/flox}$ or $p110\beta^{flox/flox}$), and no significant differences were observed between these groups.

In step 2, $Pten^{-/-}$ male mice were crossed with female $p110\alpha^{flox/flox}$ or $p110\beta^{flox/flox}$ mice, and their male offspring carrying PbCre were crossed further with $Pten^{flox/wt}$; $p110\alpha^{flox/wt}$ or $Pten^{flox/wt}$; $p110\beta^{flox/wt}$ littermates to obtain the desired $Pten^{flox/flox}$; $p110\alpha^{flox/flox}$; PbCre4 (hereafter termed '$Pten^{-/-}$; $p110\alpha^{-/-}$') or $Pten^{flox/flox}$; $p110\beta^{flox/flox}$; PbCre4 (hereafter termed '$Pten^{-/-}$; $p110\beta^{-/-}$') compound strains. The resultant $Pten^{flox/flox}$; $p110\alpha^{flox/flox}$; PbCre4 or $Pten^{flox/flox}$; $p110\beta^{wt/wt}$; PbCre4 mice from the same litters displayed high-grade prostatic intraepithelial neoplasia comparable to that of $Pten^{flox/flox}$; PbCre4 mice described in step 1, and were used interchangeably as tumour controls. Cohorts of littermates lacking the probasin Cre transgene were used as wild-type controls showing no significant differences from wild-type controls in step 1.

Alternatively, in step 2 $Pten^{-/-}$; $p110\alpha^{-/-}$ or $Pten^{-/-}$; $p110\beta^{-/-}$ males were crossed with female littermates of $Pten^{flox/lox}$; $p110\alpha^{flox/lox}$ or $Pten^{flox/flox}$; $p110\beta^{flox/flox}$ to generate larger numbers of the desired compound strains. No differences were seen in phenotypes in compound animals generated by either version of step 2.

Primary and immortalized MEFs. MEFs were prepared from embryos derived from intercrossing $p110\beta^{flox/+}$ heterozygotes at embryonic day 13.5 after fertilization. Primary WT or floxed MEFs, and DNp53 immortalized WT or floxed MEFs were treated with Ade-Cre to generate WT control and *p110β*-null (βKO) cells. Additional control cells used in our study were floxed MEFs without Ade-Cre treatment. βKO+β and βKO+KR lines were generated by introducing either HA-tagged WT human *p110β* or a kinase-inactive mutant K805R into βKO MEFs and then treated with Ade-Cre. Genotyping of MEFs was done by PCR using primer sets: LLF with LLR, and SLF with LLR (Supplementary Fig. 1).

Growth factors and western blotting. Cells were starved either for 2 h or overnight followed by stimulation with insulin (2.5 μg ml^{-1}; Sigma I2767), EGF (10 ng ml^{-1}; Sigma E9644), IGF1 (5 ng ml^{-1}, Upstate 01-208), LPA (10 μM; Sigma L7260) or 10% FBS for various periods as indicated in the corresponding figures. Western blot assays were performed as described previously[8] with antibodies against PTEN (no. 9552), p110α (no. 4255), phospho-Akt (Ser 473 (no. 9271) or Thr 308, no. 9275), Akt (no. 9272), phospho-p70 S6 kinase (Thr 389, no. 9205), phospho-p44/42 MAP kinase (no. 9101), phospho-S6 ribosomal protein (Ser 235/Ser 236, no. 2211) and S6 ribosomal protein (no. 2217) (Cell Signalling), p85 (Upstate 06-195), p110β (Santa Cruz, sc-602), Tubulin and Vinculin (Sigma T6199 and V9131). Immunofluorescently labelled anti-mouse IgG (Rockland Immunochemicals 610-132-003) and anti-rabbit IgG (Molecular Probes) were used to visualize western blots on an Odyssey scanner. The quantification of western blots was performed with Odyssey software version 2.0.

Growth curves. MEFs were seeded in 12-well tissue culture plates and stained with crystal violet at each indicated time point. The dye was extracted with 10% acetic acid followed by plate reading at 590 nm. The values were normalized to the absorbance at day 0. Data shown are the average of at least two independent experiments.

Cell cycle analysis. Cells were synchronized by starvation in DMEM supplemented with 0.1% FBS for 48 h before being released into the cell cycle by stimulation with 10% FBS. Cells were pulse-labelled with BrdU at each indicated time point and analysed in accordance with the manufacturer's protocol (BD Biosciences).

Focus formation assays. MEFs at 40–50% confluence were infected with various retroviruses: pBabe–Vector, pBabe–HRas-G12V or pBabe–EGFR-Del (ΔL747–E749, A750P) and then cultured for 14–21 days for WT, βKO+β and βKO+KR cells, but for 30–40 days for βKO cells. Confluent monolayers with foci were fixed in ethanol and stained with crystal violet.

Histology and immunohistochemistry. Prostate tissues were processed and stained as described previously[32]. Primary antibody used in immunohistochemistry was directed against phospho-Akt (Ser 473) (no. 3787, Cell Signalling).

Lipid kinase assays. *In vitro* lipid kinase assays were performed as described previously[8,18]. In brief, anti-p110β (Santa Cruz) immunoprecipitates from freshly prepared cell lysates were subjected to an *in vitro* lipid kinase assay with phosphatidylinositol (Avanti Polar Lipids) as the substrate. The phosphorylated lipids were resolved by thin-layer chromatography, detected by autoradiography and quantified with Adobe Photoshop.

Transferrin internalization assays. Cells were seeded on 10% poly-(L-lysine)-coated coverslips and grown overnight in DMEM medium supplemented with 10% FBS. The assay was performed as described previously[33] with Alexa Fluor555-conjugated human transferrin (Invitrogen), counterstained with 4,6-diamidino-2-phenylindole (1 μg ml^{-1}; Sigma) and mounted with mounting medium (Fisher Scientific). Cells were observed with a Zeiss confocal microscope LSM510META/NLO at ×63 magnification, and images were captured with Zeiss confocal microscope software 3.2.

Laser capture microdissection and DNA extraction. Laser capture microdissection was performed as described previously[34]. Genomic DNA of microdissected prostate epithelium was extracted with phenol/chloroform before PCR analysis.

Quantitative reverse transcription PCR analysis. Liver total RNAs were extracted with the use of the RNeasy kit (Qiagen). The following gene expression assay probes (Applied Biosystems) were used for real-time RT–PCR quantification: *phosphoenolpyruvate carboxykinase 1* (*PEPCK/Pck1*, ID no. Mm00440636_m1), *glucose-6-phosphatase* (*G6Pase*, ID no. Mm00839363_m1), *fructose bisphosphatase 1* (*Fbp1*, ID no. Mm00490181_m1), *hepatic nuclear factor 4* (*Hnf4a*, ID no. Mm00433964_m1) and *glyceraldehyde-3-phosphate dehydrogenase* (*GAPDH*, catalogue no. 4352339E). Expression was normalized to mRNA for *GAPDH* and results were expressed as fold change in mRNA compared with the indicated control mice.

31. Taniguchi, C. M. *et al.* Divergent regulation of hepatic glucose and lipid metabolism by phosphoinositide 3-kinase via Akt and PKCλ/ζ. *Cell Metab.* **3**, 343–353 (2006).
32. Graner, E. *et al.* The isopeptidase USP2a regulates the stability of fatty acid synthase in prostate cancer. *Cancer Cell* **5**, 253–261 (2004).
33. Sever, S., Damke, H. & Schmid, S. L. Dynamin:GTP controls the formation of constricted coated pits, the rate limiting step in clathrin-mediated endocytosis. *J. Cell Biol.* **150**, 1137–1148 (2000).
34. Emmert-Buck, M. R. *et al.* Laser capture microdissection. *Science* **274**, 998–1001 (1996).

CORRIGENDUM

doi:10.1038/nature16543

Corrigendum: Essential roles of PI(3)K–p110β in cell growth, metabolism and tumorigenesis

Shidong Jia, Zhenning Liu, Sen Zhang, Pixu Liu, Lei Zhang, Sang Hyun Lee, Jing Zhang, Sabina Signoretti, Massimo Loda, Thomas M. Roberts & Jean J. Zhao

Nature **454,** 776–779 (2008); doi:10.1038/nature07091

In Fig. 3b of this Letter we inadvertently used the wrong images (partial duplicates of images representing *p110α*$^{-/-}$ mice) in the panels representing *p110β*$^{-/-}$ mice. The corrected Fig. 3b is shown in Fig. 1 of this Corrigendum. The conclusions of the paper are not affected; knocking out either *p110α* or *p110β* does not affect the growth of the normal prostate.

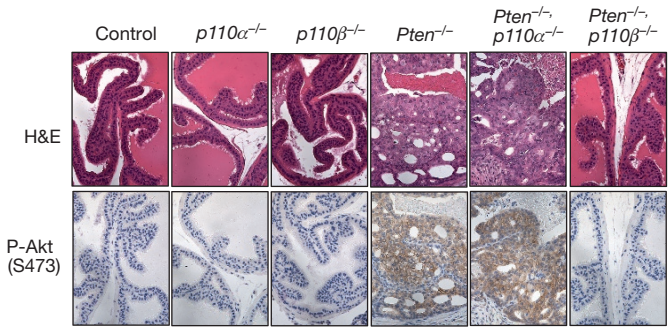

Figure 1 | This figure shows the corrected Fig. 3b of the original Letter.